

RSC Advances



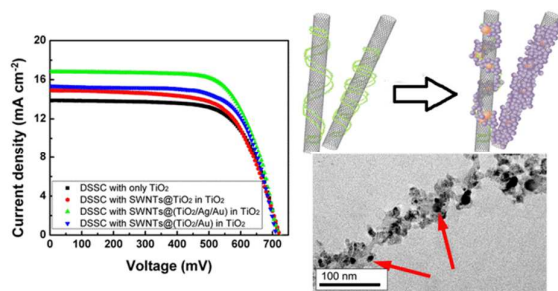
This is an *Accepted Manuscript*, which has been through the Royal Society of Chemistry peer review process and has been accepted for publication.

Accepted Manuscripts are published online shortly after acceptance, before technical editing, formatting and proof reading. Using this free service, authors can make their results available to the community, in citable form, before we publish the edited article. This *Accepted Manuscript* will be replaced by the edited, formatted and paginated article as soon as this is available.

You can find more information about *Accepted Manuscripts* in the [Information for Authors](#).

Please note that technical editing may introduce minor changes to the text and/or graphics, which may alter content. The journal's standard [Terms & Conditions](#) and the [Ethical guidelines](#) still apply. In no event shall the Royal Society of Chemistry be held responsible for any errors or omissions in this *Accepted Manuscript* or any consequences arising from the use of any information it contains.

Table of content



Based on multi-functional DNA templates, SWNTs@(TiO₂/Ag/Au) nanocomposites were synthesized to enhance the light-harvesting and charge collection efficiency of DSSCs.

ARTICLE

Multi-functional DNA-based synthesis of SWNTs@(TiO₂/Ag/Au) nanocomposites for enhanced light-harvesting and charge collection in DSSCs

Cite this: DOI: 10.1039/x0xx00000x

Received 00th January 2012,
Accepted 00th January 2012

DOI: 10.1039/x0xx00000x

www.rsc.org/

Mei Yu, Jindan Zhang, Songmei Li, Yanbing Meng and Jianhua Liu*

The performances of photovoltaic devices can be improved by increasing light-harvesting and charge collection respectively. The design and synthesis of nanocomposites with the ability of enhancing the generation and collection of the photo-generated electrons provide a significant way to improve the power conversion efficiency (PCE). Herein, SWNTs@(TiO₂/Ag/Au) nanocomposites were synthesized and successfully integrated into photoanode films of dye-sensitized solar cells (DSSCs) to improve the power conversion efficiency. The synthesis processes were based on the multi-functional DNA. DNA not only works as dispersing agent preventing SWNTs bundling but also as sacrificial mold assembling TiO₂, Ag and Au nanoparticles on the surface of the SWNTs. The synthesized SWNTs@(TiO₂/Ag/Au) nanocomposites enhance the charge collection and light-harvesting of DSSCs simultaneously. With 2.45 wt% SWNTs@(TiO₂/Ag/Au) nanocomposites incorporating into the photoanode films, the PCE of the DSSCs increases from 6.8% to 8.3%.

Introduction

There is a growing interest in the design and synthesis of nanoscale materials for various applications such as in energy or optics fields. For the thin film photovoltaic device, high efficient light-harvesting, electron collection and electron transportation are indispensable to a high efficiency photoanode.¹⁻⁴ To a specified solar cell, efficient light harvesting and electron collection require the consideration of many design criteria, including morphologies and materials.⁵ The unique surface-plasmon of nanoscale metals attracts many attentions in photo-electron field. The localized surface plasmons (LSPs) of nanoscale metals, such as Ag and Au NPs, are believed to enhance the light-harvesting of nanoporous solar cells.⁶⁻⁸ Single-walled carbon nanotubes (SWNTs) exhibit high electron mobility and their ability of increasing charge collection and transportation in photovoltaic devices has been proved.^{9,10}

Therefore, the efficient combinations of plasmonic metal particles and SWNTs, each with unique functional advantages, provide a significant way to improve the efficiency of photoanodes. And the combination can be achieved efficiently with DNA as template due to its several properties. Firstly, DNA can bind to SWNTs through π -stacking,^{11,12} preventing the bundling of SWNTs without deteriorating the electronic

properties.¹¹ Secondly, DNA is able to bond metal ions at its bases and the negatively charged phosphate groups can adsorb cations and other positively charged particles.¹³ Moreover, upon UV photoirradiation, DNA can reduce metal cations, driving the deposition of the metallization based on DNA photo-oxidation.¹⁴ Thirdly, the double-helix rigid chain structure gives DNA high mechanical strength¹⁵ and the molecular size of DNA can be easily controlled.¹⁶

Herein, a general and programmable method is demonstrated to synthesize SWNTs@(TiO₂/Ag/Au) nanocomposites using multi-functional plasmid DNA as biological template. And the resulted nanocomposites were integrated into dye-sensitized solar cells (DSSCs) to enhance power conversion efficiency (PCE). DSSCs were chosen as model application because DSSCs is one of the most representative nanoporous photovoltaic devices,¹⁷⁻¹⁹ and have a well-established mechanism theory.²⁰⁻²² After incorporating SWNTs@(TiO₂/Ag/Au) nanocomposites into the photoanode films, the PCE of the DSSCs experiences a increase from 6.8% to 8.3%. The Electrochemical Impedance spectra (EIS), UV-Vis absorption spectra and the incident photo-to-current conversion efficiency (IPCE) spectra show that the prepared SWNTs@(TiO₂/Ag/Au) nanocomposites enhance the light absorption as well as the electron collection efficiency. The

multi-functional DNA-based synthesis integrates advantages of each component part efficiently, and without performance loss.

Experimental

Synthesis of nanocomposites

100 μl plasmid DNA solution (stored in Tris-HCl and EDTA buffer, 8000 base pairs, 132 $\mu\text{g}/\text{ml}$, pH=8) was mixed with semiconducting SWNTs (50 μl , 0.1 mg/ml), and sonicated in ice for 1h to get dispersed SWNTs@DNA complexes. Then, equal molar of silver nitrate (AgNO_3 , Beijing Chemical Works) and Chloro(trimethylphosphine)gold(I) (Me_3PAuCl , Aladdin) were added into the SWNTs@DNA complexes, the molar ratio of each metal ion to the number of the plasmid base pairs is 1. The mix solution was kept in dark room at 4 $^\circ\text{C}$ overnight. After that, TiO_2 nanoparticles with diameter of 5~10 nm were added and the pH value was adjusted to ~5 with chlorhydric acid, the weight ratio of TiO_2 to the SWNTs is 10. After incubated in dark room at 4 $^\circ\text{C}$ for 6 h, the solution was irradiated by UV-C (254 nm) light for 1h with intensity of 50-80 $\mu\text{W}/\text{cm}^2$. The synthesized SWNTs@($\text{TiO}_2/\text{Ag}/\text{Au}$) composites were collected by centrifuged and washed with ethanol, then dried for subsequent use. The weight ratios of SWNTs: TiO_2 :Ag: Au in each samples are 2:20:0.9:1.6 for SWNTs@($\text{TiO}_2/\text{Ag}/\text{Au}$) nanocomposites, 2:20:0.9:0 for SWNTs@(TiO_2/Ag) nanocomposites, and 2:20:0:0 for SWNTs@ TiO_2 nanocomposites.

The morphology of templated nanocomposites were observed on lacey support films by Transmission electron microscope (TEM, JSM 2100F) under 200 KV. The UV-visible (UV-Vis) spectra were measured at room temperature on a Cintra 10e spectrometer with 1 cm quartz cuvette holders for liquid samples. The solutions for UV-Vis spectra were diluted to total volume of 3ml.

Assembly of DSSCs

The synthesized nanocomposites were mixed with commercial TiO_2 paste (average size of 20 nm, P25) through stirring and sonication repeatedly. The percentage composition of the SWNTs@ TiO_2 , SWNTs@(TiO_2/Ag) and SWNTs@($\text{TiO}_2/\text{Ag}/\text{Au}$) nanocomposites (compared to P25 TiO_2) are 2.20 wt%, 2.29 wt% and 2.45 wt%, respectively. The arrangement of the percentage composition of each nanocomposites is aimed at equaling the net content of SWNTs in each sample. The fabrication of DSSCs was carried out using a procedure from the literature.⁹ Differently, the compact n-type layer of TiO_2 between substrate and TiO_2 was achieved by spin-coating 0.1 M Titanium(IV) isopropoxide in isopropanol solution, and sintered at 450 $^\circ\text{C}$ for 30 min. The photoanodes with nanocomposites were annealed at 500 $^\circ\text{C}$ in argon gas to protect the SWNTs from burning, and then kept the photoanodes in air at 300 $^\circ\text{C}$ for 30min to remove the ethyl cellulose and terpinol in the paste.

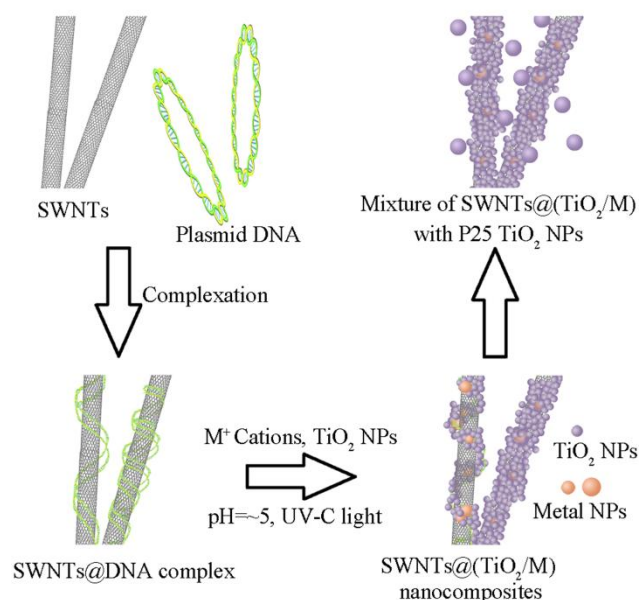
Characterization

The photovoltaic measurements were performed using an AM 1.5 solar simulator (500 W xenon lamp, NBeT, Solar-500) with an intensity of 100 mW/cm^2 , the power was calibrated by using a reference silicon photodiode with a power meter (AULIGHT, CEL-NP2000-2). The photocurrent-voltage (J-V) curves were recorded using a Keithley model 2400 source measurement unit. The incident photo-to-current conversion efficiency (IPCE) values were determined using a system comprising a monochromator, a 500 W xenon lamp, a calibrated silicon photodetector and a power meter. The Electrochemical impedance spectroscopy (EIS) spectra of DSSCs were measured using electrochemical work station (Princeton 2273, USA). The obtained EIS spectra were fitted with Z-view software. The spectra were measured at various forward bias voltages (from -0.75 to -0.5 V) in the frequency range 1 Hz to 100 kHz with oscillation potential amplitudes of 10 mV at room temperature. The photoanode was connected to the working electrode. The platinum electrode was connected to the auxiliary electrode and the reference electrode. The impedance measurements were carried out in dark conditions. The transmission line model was used for fitting the electrochemical impedance data (see Supplementary Information). The dye loading of the photoanode was determined by eluting the N719 dye from the TiO_2 electrode into 3ml of 0.1 M KOH and using a UV-vis calibration curve to determine the concentration of dye in solution to total amount of dye per square centimetre.

Results and discussion

Synthesis of SWNTs@($\text{TiO}_2/\text{Ag}/\text{Au}$) nanocomposites

Scheme 1 presents the synthesis of SWNTs@($\text{TiO}_2/\text{Ag}/\text{Au}$) based on plasmid DNA. In the first step in synthesizing SWNTs@($\text{TiO}_2/\text{Ag}/\text{Au}$) nanocomposites, SWNTs@DNA complexes was fabricated. Ag(I), Au(I) cations and TiO_2 NPs were then absorbed onto the complexes, after UV-C irradiation, Ag and Au NPs generated. It is known that DNA can bond and disperse SWNTs through π -stacking, resulting in stable helical wrapping to the surface of SWNTs@DNA complexes.^{11,12} The interaction between DNA base and metal cations leads to the insertion of M(I) to DNA at base pairs, and the negative charged phosphate backbone can bind positive charged NPs via electrostatic interactions.¹³ In acidic condition, the TiO_2 NPs shows positive electricity,²³ which causes the formation of plasmid DNA/Ag(I)/Au(I)/ TiO_2 complexes on the surface of SWNTs. The difference in bonding sites between TiO_2 NPs and Ag(I)/Au(I) cations and the large amounts of TiO_2 NPs (mole ratio of TiO_2 to Ag(I)/Au(I) cations is 13.6) ensure that Ag(I)/Au(I) cations are wrapped by TiO_2 NPs. With UV-C irradiation, photooxidations happens to plasmid DNA, and the Ag(I)/Au(I) cations capture the transferred electrons becoming Ag/Au NPs in-situ.¹⁴ The wrapping of TiO_2 avoids metal NPs from contacting the dye and the electrolyte directly, and preventing the recombination and back reaction of photogenerated carriers.²⁴



Scheme 1 Schematic representation of the fabrication of SWNTs@(TiO₂/M) nanocomposites.

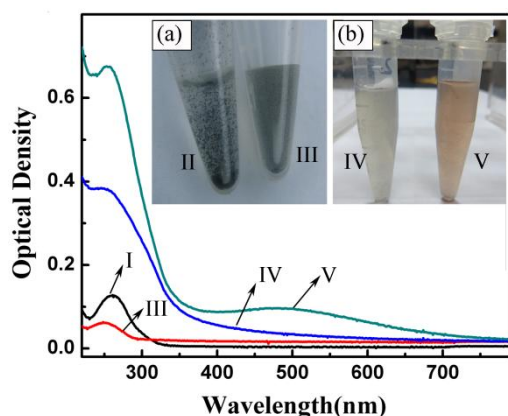


Fig. 1 UV-Vis absorption spectra of fabrication processes of SWNTs@(TiO₂/Ag/Au). Curve (I) is DNA, curve (III) is SWNTs@DNA, curve (IV) is SWNTs@TiO₂ nanocomposites and curve (V) is SWNTs@(TiO₂/Ag/Au) nanocomposites. Insets are Optical image of SWNTs in alcohol (II), SWNTs@DNA solution (III), SWNTs@TiO₂ nanocomposites solution (IV) and SWNTs@(TiO₂/Ag/Au) nanocomposites (V).

Compared to other methods for making CNT/TiO₂^{25,26} or CNT/M^{27,28} complexes, the DNA-enabled assemble method has several advantages. Firstly, SWNTs are bound and stabilized by non-covalent binding, so no chemical modification are required, preserving the high electron mobility of the SWNTs. Secondly, the DNA has a large number of active sites to interact with metal cations and other charged NPs, which can bond TiO₂ and metal cations on the surface of SWNTs. And DNA works as reduction agent and the template during the in-situ generation process of metal NPs. As a consequence, the application of the multi-functional DNA makes the method of synthesis appointed nanocomposites to be simple. And the whole process is no requirement of additive agents, which may affects the properties in application.

In UV-Vis absorption spectra (Figure 1a), the DNA absorption band at ~260 nm¹⁴ experiences a decrease in intensity due to the interaction with SWNTs, indicating the formation of the SWNTs@DNA complex. The dispersion of SWNTs induced by plasmid DNA can be clearly observed in the optical image (inset (a) in Figure 1). The SWNTs@DNA solution is homogeneous suspension while the SWNTs solution shows many granular aggregates. The UV-Vis absorption band from 400nm to 600 nm in curve belonging to SWNTs@(TiO₂/Ag/Au) indicates the generation of Ag and Au NPs.^{5,14} And the phenomenon can be observed in macroscopic image (inset (b) in Figure 1). The colour of the composites solution change from transparent colour (colour of SWNTs@TiO₂ solution) to pink (colour of SWNTs@(TiO₂/Ag/Au) solution) due to the participation of metal NPs.

TEM images of SWNTs@DNA complexes are shown in Figure 2a and 2b. The plasmid DNA wrap around SWNTs can be seen in Figure 2b. The SWNTs are bonded by plasmid DNA and well dispersed. Figure 2c is the TEM image of SWNTs@TiO₂ nanocomposites. The wire-like structure confirms that TiO₂ NPs (with diameter of 5~10 nm) are fixed by the plasmid DNA (and cover the surface of SWNTs). Similarly, SWNTs@(TiO₂/Ag/Au) nanocomposites are wire-like structure, and both TiO₂ and Ag/Au NPs are fixed on the surface of SWNTs (Figure 2d and 2e). The arrows in Figure 2e point to the Ag/Au NPs, and the TiO₂ NPs packs around the Ag/Au NPs forming a protective shell (enlarged view in Figure 2f). The TiO₂ protective shell prevents Ag/Au NPs from promoting electron recombination and from being etched by the electrolyte. The synthesized Ag and Au NPs is 5~20 nm. And the nonuniform size of the metal NPs cause the broad band (from 400 to 600 nm) in UV-Vis spectrum (Figure 1a). Both the anatase TiO₂ and FCC Ag/Au can be observed in SAED pattern (Figure 2g). The crystal structures of Ag and Au have little difference to differentiate in SAED pattern, however, the EDX spectrum (Figure 2h) and UV-Vis spectrum of the SWNTs@(TiO₂/Ag/Au) nanocomposites indicate that both Ag and Au NPs are generated. It can be confirmed that the compositions of the nanocomposites consist of Ti, O, Ag and Au elements. And the presences of Cu and some C are due to the carbon coated copper grid used for the TEM and EDX analysis.

Effect of the SWNTs@(TiO₂/Ag/Au) nanocomposites

To investigate the effect of the SWNTs@(TiO₂/Ag/Au) nanocomposites on the performance of the DSSCs, SWNTs@(TiO₂/Ag/Au) nanocomposites were incorporated into the DSSCs. DSSCs with only TiO₂ as photoanodes, with SWNTs@TiO₂ and with SWNTs@(TiO₂/Ag) incorporated are used as controls. The thickness of each photoanode films is about 13 μm (Figure S1). Figure 3 shows the J-V curves of the different kinds of DSSCs. The related photovoltaic parameters (short-circuit current density (J_{sc}), open circuit voltage (V_{oc}), fill factor (FF), power conversion efficiency (PCE), electron collection efficiency (η_{COL}) and dye loading) are summarized in Table 1. The DSSCs with SWNTs@TiO₂ nanocomposites pres-

ARTICLE

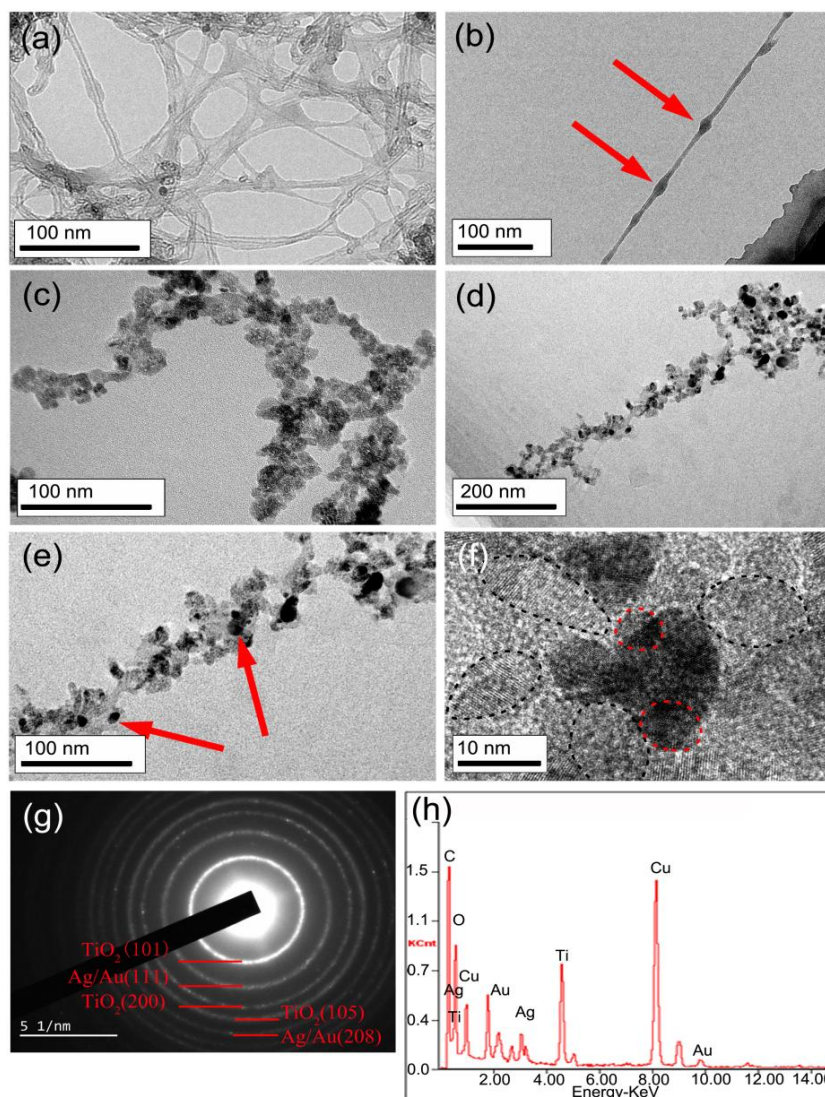


Fig. 2 TEM images of SWNTs@DNA complexes (a) and (b). (c) is TEM image of SWNT@TiO₂ nanocomposites. (d) and (e) are TEM images of SWNTs@(TiO₂/Ag/Au) nanocomposites. (f)~(h) HRTEM image, SAED pattern and EDX spectrum of SWNTs(TiO₂/Ag/Au) nanocomposites.

ents a PCE of 7.1% and a J_{sc} of 14.9 mA/cm², which are higher than those of the DSSCs with TiO₂-only (6.8% and 13.9 mA/cm²). The improvement of the efficiency can be attributed to the high charge collection induced by the SWNTs. Compared with the DSSCs with SWNTs@TiO₂, DSSCs with SWNTs@(TiO₂/Ag/Au) have an improvement in the PCE and the J_{sc} (8.3% and 16.8 mA/cm²). And that is caused by the incorporating of the Ag/Au NPs, it can be inferred that the LSPs of Ag/Au NPs enhance the efficiency of the DSSCs.

The PCE and J_{sc} of DSSCs with SWNTs@(TiO₂/Ag) nanocomposites (7.6% and 15.4 mA/cm²) are higher than

SWNTs@TiO₂ sample, while lower than those of the DSSCs with SWNTs@(TiO₂/Ag/Au). The differences in performance can be related to the introduction of Au nanoparticles. It is known that the LSPs of Au can be induced by the 570 nm light, and for Ag is 450 nm. Thus, the incorporation of Au and Ag can make panchromatic solar energy conversion (visible light).

The dye loading data in Table 1 shows that the incorporating nanocomposites can improve the dye loading to a certain extent compared with the 20 nm TiO₂-only sample. It may be related to the incorporation of the 5 nm TiO₂ (2 wt%).

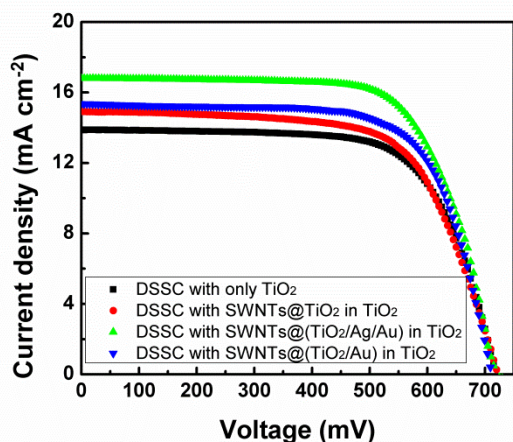


Fig. 3 J-V curves of DSSC with TiO₂ only, DSSC with SWNTs@TiO₂, DSSC with SWNTs@(TiO₂/Ag/Au) and DSSC with SWNTs@(TiO₂/Ag). The curves were obtained under AM 1.5G simulated sunlight with a power density of 100 mW cm⁻². The active area of the photoanode was 0.2 cm².

Table 1 Photovoltaic parameters of DSSC with TiO₂ only, DSSC with SWNTs@TiO₂, DSSC with SWNTs@(TiO₂/Ag/Au) and DSSC with SWNTs@(TiO₂/Ag)

Sample DSSCs	J_{sc} (mA cm ⁻²)	V_{oc} (mV)	FF (%)	PCE (%)	η_{COL} (%)	Dye loading (10 ⁻⁷ mol cm ⁻²)
20 nmTiO ₂ -only	13.9	717	68.7	6.8	94.0	1.62
SWNTs@TiO ₂	14.9	722	66.0	7.1	99.8	1.80
SWNTs@(TiO ₂ /Ag/Au)	16.8	722	69.7	8.3	99.7	1.81
SWNTs@(TiO ₂ /Ag)	15.4	715	70.2	7.8	99.7	1.80

The smaller size TiO₂ makes the material have larger specific surface area (more detail data seen in supplementary information). However, the photoanodes with SWNTs@TiO₂, SWNTs@(TiO₂/Ag) and SWNTs@(TiO₂/Ag/Au) have attached similar amount of dye. The dye loading impact can be excluded when do the comparison among the three samples. Thus, in consideration of the components and structures of the SWNTs@(TiO₂/Ag/Au) nanocomposites, the enhancement of the PCE due to the incorporation of the SWNTs@(TiO₂/Ag/Au) nanocomposites can be concluded as two aspects except for dye loading difference: improvements of the carrier collection efficiency and increase of the light-harvesting.

To demonstrate the effects of the SWNTs@(TiO₂/Ag/Au) nanocomposites on the electron diffusion length (L_n) and the η_{COL} of photoanodes in DSSCs, the EIS spectra were measured under dark condition at various forward bias (Figure 4b). The data of the calculated L_n/L (L is the photoanode thickness) are presented in Figure 4c. The EIS were fitted using transmission line model (Figure 4a),¹⁹⁻²² and the details of the calculation of L_n/L and η_{COL} are provided in supplementary information. The values of the extrapolated diffusion length can indicate the difference in electron collection efficiency²⁰ (see in supplementary information). The DSSCs with SWNTs@(TiO₂/Ag/Au) nanocomposites show longer L_n (~10.6

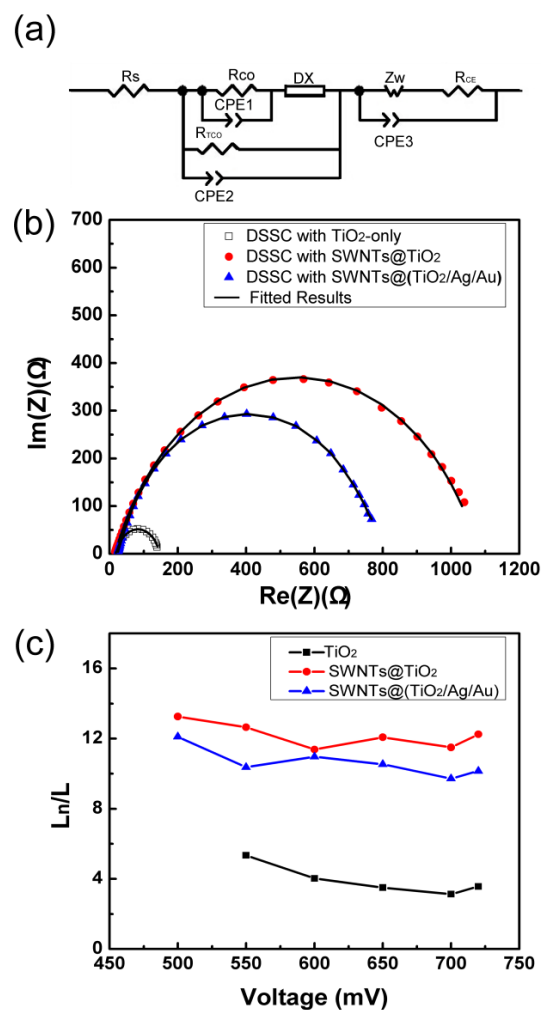


Fig. 4 Equivalent circuit impedance model (a), EIS spectra (b) and calculated electron diffusion length (c) of DSSCs. In the equivalent circuit, R_s is the series resistance. R_{co} and CPE1 are the contact resistance and capacitance at the interface between the FTO and the TiO₂ photoanode film. R_{rco} and CPE2 are the charge transfer resistance and the interface capacitance at the uncovered layer of FTO to the electrolyte. Z_w is the mass transport impedance at the counter electrode. R_{ce} and CPE3 charge transfer resistance and double layer capacitance at the counter electrode/electrolyte interface.

times the film thickness) and higher η_{COL} (99.7%) than that of the TiO₂-only DSSCs (~3.9 times, 94.0%). These results confirm that the incorporation of SWNTs@(TiO₂/Ag/Au) improves the electron collection and transportation.

The L_n is enhanced because the conduction band of the semiconducting SWNTs is lower than that of TiO₂ and thus, the photogenerated electrons transfer from the TiO₂ NP to the SWNTs in the SWNTs@(TiO₂/Ag/Au) nanocomposites spontaneously.⁹ Then the SWNTs quickly transfer the electrons to the fluorine-doped tin oxide (FTO), preventing back electron transfer and recombination. Compared with the high L_n (~12.3 times film thickness) of SWNTs@TiO₂ incorporated photoanode, the SWNTs@(TiO₂/Ag/Au) incorporated photoanode decreases from 12.3 to 10.6. That shows the introduction of Ag and Au NPs decreases the L_n/L value and the η_{COL} (from 99.8% to 99.7%). The decrease may be attribut-

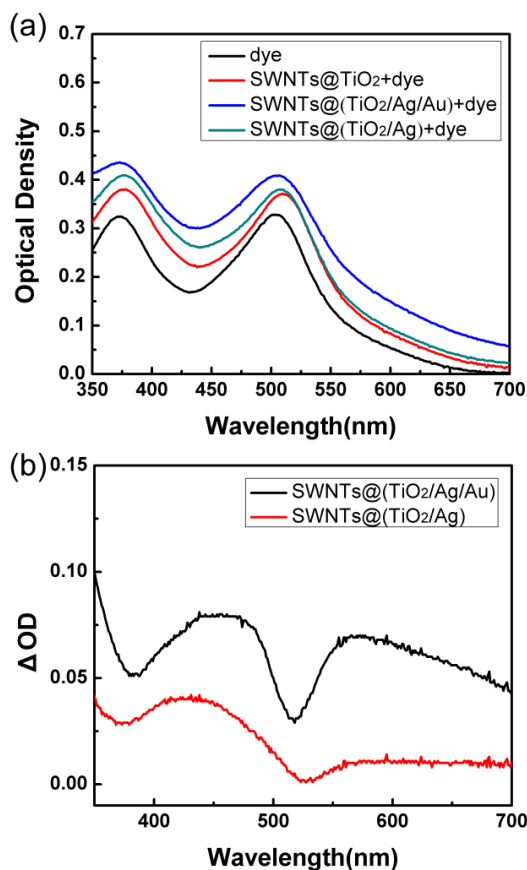


Fig. 5 (a) Optical absorptions of dye molecules (N719) and nanocomposites enhancement in solution. (b) Net changes of dye absorption (ΔOD) due to the presences of SWNTs@ $(TiO_2/Ag/Au)$ and SWNTs@ (TiO_2/Ag) compared with SWNTs@ TiO_2 +dye solution. $\Delta OD_{(SWNTs@(TiO_2/Ag/Au))}(\lambda) = OD_{(SWNTs@(TiO_2/Ag/Au)+dye)}(\lambda) - OD_{(SWNTs@TiO_2)}(\lambda)$, and $\Delta OD_{(SWNTs@(TiO_2/Ag))}(\lambda) = OD_{(SWNTs@(TiO_2/Ag)+dye)}(\lambda) - OD_{(SWNTs@TiO_2)}(\lambda)$.

ed to increasing electron-hole recombination induced by the metal NPs, decreasing the number of carriers available for photocurrent generation.²⁹ However, compared with TiO_2 -only DSSCs the L_n/L value and η_{COL} of the SWNTs@ $(TiO_2/Ag/Au)$ incorporated DSSCs still remain high.

The effect of SWNTs@ $(TiO_2/Ag/Au)$ nanocomposites on absorption of dye solution was investigated (Figure 5a). Compared with pure dye solution, the SWNTs@ $(TiO_2/Ag/Au)$ nanocomposites enhance the dye absorption over the entire wavelength range (400-700 nm). The net enhancements (ΔOD) from impacts of Ag/Au NPs LSPs were obtained through subtracting the effects of SWNTs on the dye absorption (Figure 5b). The ΔOD curve shows two clearly peaks around 450 nm and 570 nm, which can be related to the LSPs of Ag^{6,24} and Au^{5,8} impacts, respectively. As a contrast, however, the band which belongs to Au influence does not show in the curve of $\Delta OD_{(SWNTs@(TiO_2/Ag))}$. The results confirm that the LSPs of the noble metal (Ag and Au) in the nanocomposites has the ability of improving the light absorption of dyes as single metal NPs do in literature.^{5-8,24}

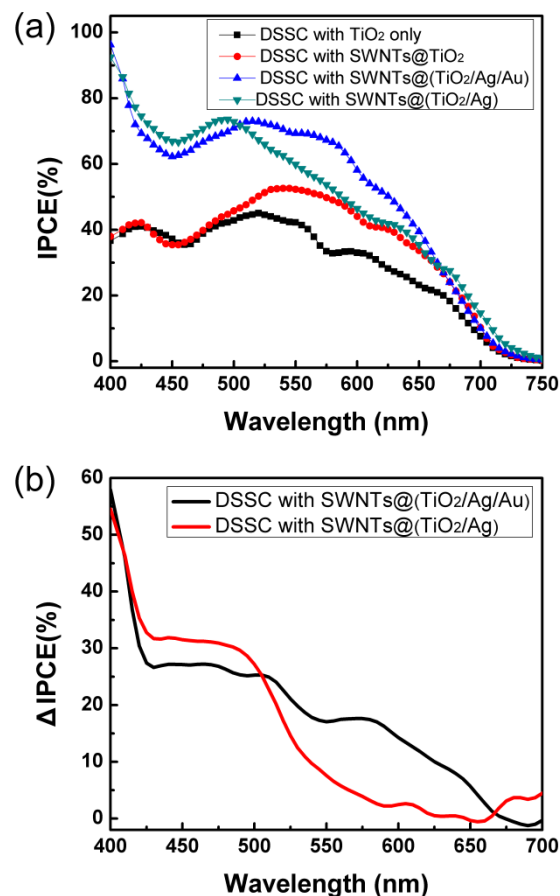


Fig. 6 (a) IPCE spectra of the DSSC with TiO_2 only, DSSC with SWNTs@ TiO_2 , DSSC with SWNTs@ $(TiO_2/Ag/Au)$, and DSSC with SWNTs@ (TiO_2/Ag) ; the net changes of the IPCE caused by the incorporation of SWNTs@ $(TiO_2/Ag/Au)$, and SWNTs@ (TiO_2/Ag) . $\Delta IPCE_{(DSSC \text{ with } SWNTs@(TiO_2/Ag/Au))}(\lambda) = IPCE_{(DSSC \text{ with } SWNTs@(TiO_2/Ag/Au))}(\lambda) - IPCE_{(DSSC \text{ with } SWNTs@TiO_2)}(\lambda)$; $\Delta IPCE_{(DSSC \text{ with } SWNTs@(TiO_2/Ag))}(\lambda) = IPCE_{(DSSC \text{ with } SWNTs@(TiO_2/Ag))}(\lambda) - IPCE_{(DSSC \text{ with } SWNTs@TiO_2)}(\lambda)$.

To clarify the effects of SWNTs@ $(TiO_2/Ag/Au)$ nanocomposites on the spectral response of solar cells, the IPCE measurement was performed (Figure 6a). Compared with TiO_2 -only DSSCs, the IPCE of the DSSCs with SWNTs@ $(TiO_2/Ag/Au)$ is increased much over the entire wavelength. The IPCE is product of the light-harvesting efficiency, electron injection efficiency, and electron collection efficiency.¹⁰ The increase of IPCE due to the incorporation of SWNTs@ TiO_2 into the DSSCs is related to enhancement of electron collection efficiency induced by the SWNTs. Moreover, the introduction of Ag and Au NPs lead to a further increase of IPCE. As shown in Figure 6b, the net changes of the IPCE caused by the incorporation of SWNTs@ $(TiO_2/Ag/Au)$ (compared to SWNTs@ TiO_2 curve, $\Delta IPCE_{(DSSC \text{ with } SWNTs@(TiO_2/Ag/Au))}$) show two main enhancements around 470 nm and 570 nm, similar as the light absorption curve. It can be concluded that the SWNTs@ $(TiO_2/Ag/Au)$ nanocomposites enhance the light absorption as well as the electron collection efficiency. The tests of the DSSCs with SWNTs@ $(TiO_2/Ag/Au)$ nanocomposites indicate that the

multi-functional plasmid DNA-based synthesis integrates advantages of each component part efficiently, and without performance loss. The synthesized SWNTs@(TiO₂/Ag/Au) nanocomposites is expected to be useful in other energy related applications, which makes this strategy versatile.

Conclusions

In summary, the SWNTs@(TiO₂/Ag/Au) nanocomposites were synthesized based on the plasmid DNA as a multi-functional biotemplate. And the synthesized nanocomposites were successfully applied to enhance the DSSC performance. A small amount (2.45 wt%) of SWNTs@(TiO₂/Ag/Au) nanocomposites improve the PCE of DSSC by ~22% (from 6.8% to 8.3%). The synthesized SWNTs@(TiO₂/Ag/Au) nanocomposites enhance the dye loading, light-harvesting as well as the electron collection efficiency. We believe that this strategy could be also applied for other thin film photovoltaic technologies that require high efficient light-harvesting, electron collection and transportation.

Acknowledgements

This work was supported by the National Natural Science Foundation of China (No. 21371019).

Notes and references

School of Materials Science and Engineering, Beihang University, Beijing 100191, China. Fax & Tel: 86-010-82317103; E-mail: liujh@buaa.edu.cn

† Electronic Supplementary Information (ESI) available: See DOI: 10.1039/b000000x/

- S. K. Pathak, A. Abate, P. Ruckdeschel, B. Roose, K. C. Gödel, Y. Vaynzof, A. Santhala, S. Watanabe, D. J. Hollman, N. Noel, A. Sepe, U. Wiesner, R. Friend, H. J. Snaith and U. Steiner, *Adv. Funct. Mater.*, 2014, in press, DOI: 10.1002/adfm.201401658.
- G. D. Sharma, D. Daphnomili, K. S. V. Gupta, T. Gayathri, S. P. Singh, P. A. Angaridis, T. N. Kitsopoulos, D. Tasise and A. G. Coutsolelos, *RSC Adv.*, 2013, **3**, 22412.
- K. C. Sun, M. B. Qadir and S. H. Jeong, *RSC Adv.*, 2014, **4**, 23223
- U. Nithiyanantham, A. Ramadoss and S. Kundu, *RSC Adv.*, 2014, **4**, 35659.
- P. Chen, X. Dang, M. T. Klug, J. Qi, N. D. Courchesne, F. J. Burpo, N. Fang, P. T. Hammond and A. M. Belcher, *ACS Nano*, 2013, **7**, 6563.
- X. Zhang, J. Liu, S. Li, X. Tan, M. Yu and J. Du, *RSC Adv.*, 2013, **3**, 18587.
- S. P. Lim, A. Pandikumar, N. M. Huang and H. N. Lim, *RSC Adv.*, 2014, **4**, 38111.
- X. Dang, J. Qi, M. T. Klug, P. Chen, D. S. Yun, N. X. Fang, P. T. Hammond and A. M. Belcher, *Nano Lett.*, 2013, **13**, 637.
- X. Dang, H. Yi, M. Ham, J. Qi, D. S. Yun, R. Ladewski, M. S. Strano, P. T. Hammond and A. M. Belcher, *Nature Nanotech.*, 2011, **6**, 377.
- X. Zhang, J. Liu, S. Li, X. Tan, J. Zhang, M. Yu and M. Zhao, *J. Mater. Chem. A*, 2013, **1**, 11070.
- M. Zheng, A. Jagota, E. D. S., B. A. Diner, R. S. Mclean, S. R. Lustig, R. E. Richardson and N. G. Tassi, *Nature Mater.*, 2003, **2**, 338.
- C. Zhao, K. Qu, Y. Song, C. Xu, J. Ren and X. Qu, *Chem. Eur. J.*, 2010, **16**, 8147.
- R.M. Izatt, J.J. Christensen and J.H. Rytting, *Chem. Rev.*, 1971, **71**, 439.
- J. Liu, X. Zhang, M. Yu, S. Li and Jindan Zhang, *Small*, 2012, **8**, 310.
- D. Wirtz, *Phys. Rev. Lett.*, 1995, **75**, 2436.
- T. X. Fan, S. K. Chow and D. Zhang, *Prog. Mater. Sci.*, 2009, **54**, 542.
- J. Bisquert, G. Garcia-Belmonte, F. Fabregat-Santiago, N. S. Ferriols, P. Bogdanoff and E. C. Pereira, *J. Phys. Chem. B*, 2000, **104**, 2287
- G. Zhang, Q. Liao, Z. Qin, Z. Zhang, X. Zhang, P. Li, Q. Wang, S. Liua and Y. Zhang, *RSC Adv.*, 2014, **4**, 39332.
- L. Yang and W. W. Leung, *RSC Adv.*, 2013, **3**, 25707.
- J. Halme, P. Vahermaa, K. Miettunen and P. Lund, *Adv. Mater.*, 2010, **22**, 210.
- M. Wang, P. Chen, R. Humphry-Baker, S. M. Zakeeruddin and M. Gratzel, *Chem. Phys. Chem.*, 2009, **10**, 290.
- J. Bisquert, F. Fabregat-Santiago, I. Mora-Sero, G. Garcia-Belmonte and S. Gimenez, *J. Phys. Chem. C*, 2009, **113**, 17278.
- T. Amano, T. Toyooka and Y. Ibuki, *Sci. Total Environ.*, 2010, **408**, 480
- J. Qi, X. Dang, P. T. Hammond and A. M. Belcher, *ACS Nano*, 2011, **5**, 7108.
- D. Eder and A. H. Windle, *Adv. Mater.*, 2008, **20**, 1787.
- P. Brown, K. Takechi and P. V. Kamat, *J. Phys. Chem. C*, 2008, **112**, 4776.
- M. Sanles-Sobrido, L. Rodriguez-Lorenzo, S. Lorenzo-Abalde, A. Gonzalez-Fernandez, M. A. Correa-Duarte, R. A. Alvarez-Puebla and L. M. Liz-Marzan, *Nanoscale*, 2009, **1**, 153.
- T. Chen, Z. Cai, L. Qiu, H. Li, J. Ren, H. Lin, Z. Yang, X. Sun and H. Peng, *J. Mater. Chem. A*, 2013, **1**, 2211.
- H. F. Zarick, O. Hurd, J. A. Webb, C. Hungerford, W. R. Erwin, and Rizia Bardhan, *ACS Photonics*, 2014, **1**, 806.